Optimal Control of a Ball Pitching Robot

Esubalewe Lakie Yedeg and Eddie Wadbro
Department of Computing Science
Umeå University
SE-901 87 Umeå, Sweden
Email: {yedegl, eddiew}@cs.umu.se

Keywords: motion planning, optimal control, underactuated system

We study a two-link pitching robot, with an active gripping mechanism and aim to make it throw a ball as far as possible. The two links are connected at the elbow joint by a linear torsional spring. The gripping mechanism is able to hold a ball and release it at any specified time. The two-link pitching robot is connected to a motor shaft at the shoulder joint by a non-linear torsional spring. The shoulder joint is held fixed at the origin of the coordinate system. The configuration of the arm and the motor shaft is illustrated in Figure 1 and described by the angels q_1 and q_m, measured with respect to the horizontal axis, respectively, whereas q_2 denote the angle change between the arm and forearm at the elbow joint.

The Euler–Lagrange formulation governing the dynamic system of the throwing robot can be written as

$$I_m \ddot{q}_m + \tau_s(q) = \tau,$$

$$M(q)\begin{bmatrix}\ddot{q}_1\\ \ddot{q}_2\end{bmatrix} + C(q,\dot{q})\begin{bmatrix}\dot{q}_1\\ \dot{q}_2\end{bmatrix} + G(q) - K(q) = 0,$$

where, I_m the motor inertia, $M(q)$ is the inertia matrix for the two-link system, $C(q,\dot{q})$ matrix of centrifugal and Coriolis forces, $\tau_s(q)$ is the torque at the shoulder joint, $G(q)$ is a vector of gravitational forces, and $K(q)$ is a vector of elastic forces.

The system has four time-global constraints limiting the set of possible control torque profiles. These constraints are (1) the absolute torque is limited to 180 Nm (2) the torque change in time is allowed to be at most 1000 Nm/s (3) the motor power bound is 270 Nm/s (4) the absolute angular velocity of the motor shaft cannot exceed 3.8717 rad/s.

Here, we aim to determine the input torque from the motor and the time t_f at which the gripping mechanism releases the ball. After the ball is released, it enters ballistic flight and hits the ground at the point $(J, 0)$. The robot pitches in the negative direction with respect to the coordinate system. So by minimizing J, we maximize the distance between the origin and the point where the ball hits the ground.

We optimize over the torque change in time and thus we include constraints on the motor torque and the torque change in time in the definition of the admissible controls. The two other constraints are replaced by approximate integral constraints for computational efficiency. We use Heun's method to discretize the state equation. We solve the nonlinear optimal control problem numerically by using an interior point method with BFGS Hessian approximation. Here, we use adjoint based gradient computation to estimate the gradients of the objective function and the state constraints.

Figure 2 shows the time evolution of the angular velocity $\dot{q}_m$ of the motor shaft and the absolute velocity $|v_b|$ of the ball. This figure illustrates that the constraint on the angular velocity is active at nearly all points in time. The only exceptions are the initial deceleration and the switch from backward to forward motion of the motor shaft, which happens after about half the total time. Figure 3 illustrates the trajectory of the ball during the optimal throwing motion. The snapshots, taken at equal time interval 0, $t_f/3$, $2t_f/3$, and t_f, suggest that more than two thirds of the total time is spend swing the ball against the throwing direction. When the ball changes direction, there is much potential energy accumulated at elbow spring that causes a rapid acceleration of the ball which obtains its maximum velocity at the release line.

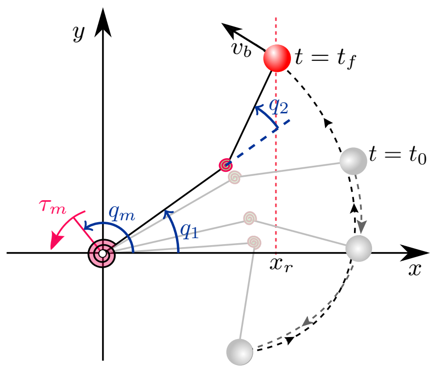

Figure 1: Configuration of the pitching robot at the release line and a possible ball trajectory.

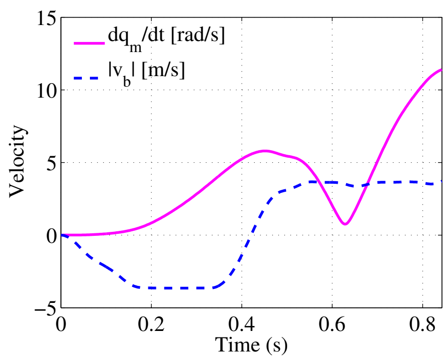

Figure 2: Time evolution of $\dot{q}_m$, the angular velocity of the motor shaft, (dashed line) and $|v_b|$, the abosolute velocity of the ball (solid line) computed using the optimal input torque.

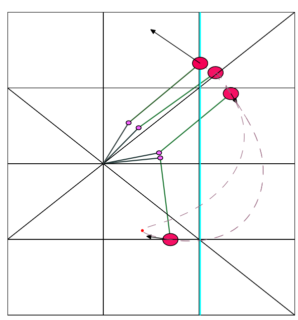

Figure 3: Illustration of the ball trajectory for the optimal input torque. The snapshots of the setup are taken at times $t = 0, t_f/3$, $2t_f/3$, and t_f.